Dynamics and Control of Microwave-Propelled Sails

C.T. Abdallah, E. Schamiloglu, K.A. Miller,* D. Georgiev,† J. Benford,‡ G. Benford,§ G. Singh, ¶

September 21, 2000

Space Technology and Applications International Forum 2001
Albuquerque, NM
February 11-15, 2001

*C.T. Abdallah, E. Schamiloglu, and K.A. Miller are with the Department of Electrical and Computer Engineering, University of New Mexico, Albuquerque, NM 87131 - contact author chaouki@eece.unm.edu
†Department of Mechanical Engineering, University of New Mexico, Albuquerque, NM 87131
‡Microwave Sciences, Inc., 1041 Los Arabis Lane, Lafayette, CA 94549
§Department of Physics and Astronomy, University of California, Irvine, 4129 Frederick Reines Hall, Irvine, CA 92697-4575
¶Jet Propulsion Laboratory,4800 Oak Grove Drive, Pasadena, California 91109

Abstract

This paper is concerned with the stability of carbon fiber sail structures that are being studied in a series of experiments at the Jet Propulsion Laboratory (JPL) by a team led by Microwave Sciences, Inc. The passive dynamic stability in the one-dimensional (1-D) case is most easily understood in terms of the fixed points of the trajectories for the governing equations of motion. A more elaborate attempt at studying the three-dimensional (3-D) stability of rigid sail configurations with a distributed mass and accounting for sail spin is also being performed using a code developed at JPL. The simple 1-D model introduces the possibility of controlling a microwave-propelled sail using various nonlinear control strategies. This work will be extended in the future to control the full 3-D case. We present results of studies in both the 1-D and 3-D analyses. In addition to providing guidance to future proof-of-principle experiments, this work will lead to novel strategies for enabling a feedback power controller to steer a sail to a desired altitude.

1 Introduction

Microwave-propelled sails belong to a class of spacecrafts that promises to revolutionize future space travel. As an example, NASA's Gossamer Spacecraft Initiative focuses on developing spacecraft architectures for very large, ultra-lightweight apertures and structures. A goal of this initiative is to achieve breakthrough enhancements in mission capability and reductions in mission cost, primarily through revolutionary advances in structures, materials, optics, and adaptive and multifunctional systems. Solar and other types of sails will provide low-cost propulsion, station-keeping in unstable orbits, and precursor interstellar exploration missions. For a general introduction to solar sails and similar structures the reader is referred to [2]. For an introduction to the notion of beamed microwave power and its application to space propulsion the reader is referred to [3]. This paper is concerned specifically with the stability and control of carbon fiber sails propelled using microwave radiation. This work is in support of ground-breaking experiments that are being performed at JPL by a team led by Microwave Sciences, Inc.

The notion of *beam-riding*, *i.e.*, the stable flight of a sail propelled by Poynting flux, places considerable demands upon a sail. Even if the beam is steady, a sail can wander off the beam if its shape becomes deformed, or if it does not have enough spin to keep its angular momentum aligned with the beam direction, in the face of perturbations. Generally, sails without structural elements cannot be flown if they are convex toward the beam, as the beam pressure would cause them to collapse. On the other hand, the beam pressure keeps concave shapes in tension, so concave shapes arise naturally while beam riding. They will resist sidewise motions if the beam moves off center, since a net sideways force restores the sail to its position. Therefore, we concentrate on a conical shape for the sail and study its dynamics in 1-D. We will illustrate that such conical shapes will oscillate in 1-D when a constant microwave power beam is used. We will then present various feedback controllers to show how to stabilize such shapes about a given height. We follow the 1-D analysis with some preliminary results of 3-D calculations of the regions of stability of rigid conical sails with a distributed mass. The sail's shape is shown in Figure 5

This paper is organized as follows: Section 2 presents the 1-D system dynamics, while section 3 discusses the various controller designs, including both the open and closed-loop cases. Section 4 presents numerical examples for the 1-D analysis. We then discuss the 3-D studies in section 5, along with some preliminary results. Section 6 summarizes our conclusions and presents directions for future research.

2 1-D Problem Statement

The problem we are concerned with is that of controlling a sail that is only allowed to move in the vertical direction, under the influence of a microwave power source placed either on earth or in orbit. The 1-D dynamics of the sail are given by [1]:

$$\frac{1}{g}\frac{d^2z}{dt^2} = -1 + \frac{P}{P_0}\frac{\cos^2\theta}{(1+\frac{z}{R}\tan\Phi)^2}, \tag{1}$$

where g is the acceleration of gravity (constant in the appropriate units), P_0 is the power necessary to overcome gravity, z is the elevation refrenced to $z = 0$, R is the beam radius, Φ is half of the total beam opening angle, and θ is the angle at which the microwave photons strike the sail. In the case of high altitudes, θ is close to zero and $\cos\theta = 1$. In addition, $\tan\Phi = 1$ and therefore, equation (1) is reduced to,

$$\frac{1}{g}\frac{d^2z}{dt^2} = -1 + \frac{P}{P_0}\frac{1}{(1+\frac{z}{R})^2}. \tag{2}$$

The equations of the sails are then written in state-space form as

$$\begin{bmatrix} \dot{x}_1 \\ \dot{x}_2 \end{bmatrix} = \begin{bmatrix} x_2 \\ -g \end{bmatrix} + \begin{bmatrix} 0 \\ \frac{g}{P_0}\frac{1}{(1+x_1/R)^2} \end{bmatrix} u \tag{3}$$

where $x_1 = z$ and $x_2 = \dot{z}$, and $u = P$.

In the case where $\cos\theta$ is not close to 1, and letting

$$\cos\theta = \frac{z^2}{z^2+r^2}$$

and averaging over the disk radius r we obtain the following dynamics,

$$\frac{1}{g}\frac{d^2z}{dt^2} = -1 + \frac{P}{P_0}\ln\left(1+\frac{R^2}{z^2}\right). \tag{4}$$

A more typical fall-off in beam power is as $P = P^*\cos^m\theta$ where $m = 1, 2, \cdots$ is used to describe different fall-off rates. In a similar fashion to the previous development, and averaging over r we obtain the following dynamics,

$$\frac{1}{g}\frac{d^2z}{dt^2} = -1 + \frac{P}{P_0}\ln\left(1+\frac{R^2}{z^2}\right). \tag{5}$$

3 Control Design

We will first recall the Poincaré-Bendixon Theorem as presented for example in [4].

Theorem 1 Poincaré-Bendixon: *let γ^+ be a bounded semiorbit of $\dot{x} = f(x)$; $x \in \mathbb{R}^2$ and let L^+ be its positive limit set. If L^+ contains no equilibrium points, then it is a periodic orbit.*

We will use this theorem to show that for a constant input power P in the system (3), there exists a closed bounded set $M \subset \mathbb{R}^2$ that is positively invariant (*i.e.*, any solution that starts in M remains in M for all later times), and does not contain any equilibrium points of (3). Then we deduce that since M is closed, the positive limit set L^+ is in M. The Poincaré-Bendixon theorem then guarantees the existence of a periodic orbit for (3).

3.1 Analysis for Constant Power P

In the case of a constant power P we will show that the trajectories will be attracted to a limit cycle as follows. Consider again the system (3) but with $u = P$ where P is a constant such that $P > P_0$. Note first that the only equilibrium point of the system (7) is at

$$x_e = \begin{bmatrix} x_{e1} \\ x_{e2} \end{bmatrix} = \begin{bmatrix} R\left[\sqrt{\frac{P}{P_0}} - 1\right] \\ 0 \end{bmatrix}. \tag{6}$$

We can re-write system (1) as:

$$\begin{bmatrix} \dot{x}_1 \\ \dot{x}_2 \end{bmatrix} = \begin{bmatrix} x_2 \\ -g + g\frac{P}{P_0}\frac{1}{(1+x_1/R)^2} \end{bmatrix}. \tag{7}$$

Then, let us consider a Lyapunov function candidate

$$V(x_1, x_2) = \frac{1}{2}x_2^2 + \int_{x_{e1}}^{x_1} \left[g - g\frac{P}{P_0}\frac{1}{(1+w/R)^2} \right] dw. \tag{8}$$

Note first that for all $w \in [x_{e1}, x_1/R]$, the integrand is non-negative and thus $V(x_1, x_2)$ is a Lyapunov function candidate, *i.e.*, V is positive definite. Then let us compute the time derivative of V along the trajectories of (7),

$$\begin{aligned} \dot{V}(x) &= x_2\dot{x}_2 + \left[g - g\frac{P}{P_0}\frac{1}{(1+x_1/R)^2} \right] \dot{x}_1 \\ &= x_2\dot{x}_2 - \dot{x}_1\dot{x}_2 \\ &= 0. \end{aligned} \tag{9}$$

Thus, the trajectories of (7) can not cross the level surfaces $V(x) = c$ for any positive constant c. Now consider the set

$$M = \{x \in \mathbb{R}^2; \mathrm{c_1} \le \mathrm{V(x)} \le \mathrm{c_2}\} \tag{10}$$

for any $0 < c_1 < c_2$. Note that M is bounded and positive invariant. On the other hand, recall that the only equilibrium point of the system (7) is at

$$x_e = \begin{bmatrix} R\left[\sqrt{\frac{P}{P_0}} - 1\right] \\ 0 \end{bmatrix}. \tag{11}$$

This equilibrium point is outside the set M since $V(x_e) = V(x_{e1}, 0) = 0$. Thus, calling on the Poincaré-Bendixon theorem, we conclude that M contains a periodic orbit. Moreover, we will show next that this periodic orbit is stable.

Note that a similar discussion may be used to show that (5) has a limit cycle with the choice of

$$V(x_1, x_2) = \frac{1}{2}x_2^2 + \int_{x_{e1}}^{x_1} \left[g - g\frac{P}{P_0}\ln(1 + \frac{R^2}{w^2}) \right] dw \tag{12}$$

where $x_{e1} = R\sqrt{e^{P/P_0}}$.

3.2 Feedback Control Design

In this subsection, we present two families of nonlinear control designs which can guarantee the closed-loop stability of the sails.

3.2.1 Lyapunov-based design

Let us consider the feedback control design problem for a general form of our system

$$\begin{bmatrix} \dot{x}_1 \\ \dot{x}_2 \end{bmatrix} = \begin{bmatrix} x_2 \\ -g \end{bmatrix} + \begin{bmatrix} 0 \\ G(x) \end{bmatrix} u,$$

where $x_1 = z$, $x_2 = \dot{z}$, and $u = P$. The term $G(x)$ denotes either $\frac{g}{P_0(1+x_1/R)^2}$ or $\frac{g}{P_0}\ln\left(1 + \frac{R^2}{z^2}\right)$. Note that in either case $G(x)$ can never be zero as long as $x_1 \ge 0$. We will use a very general approach to design u using Lyapunov functions. To this end, consider a scalar function $V(x)$ that is positive definite, *i.e.*, $V(x) > 0$, $\forall\, x \ne 0$ and $V(0) = 0$. Then let us look at its time derivative,

$$\begin{aligned} \dot{V}(x) &= \frac{\partial V(x)}{\partial x}\dot{x} \\ &= \begin{bmatrix} \frac{\partial V(x)}{\partial x_1} & \frac{\partial V(x)}{\partial x_2} \end{bmatrix} \begin{bmatrix} \dot{x}_1 \\ \dot{x}_2 \end{bmatrix} \\ &= \frac{\partial V(x)}{\partial x_1}x_2 + \frac{\partial V(x)}{\partial x_2}\left[-g + G(x)u\right]. \end{aligned} \tag{13}$$

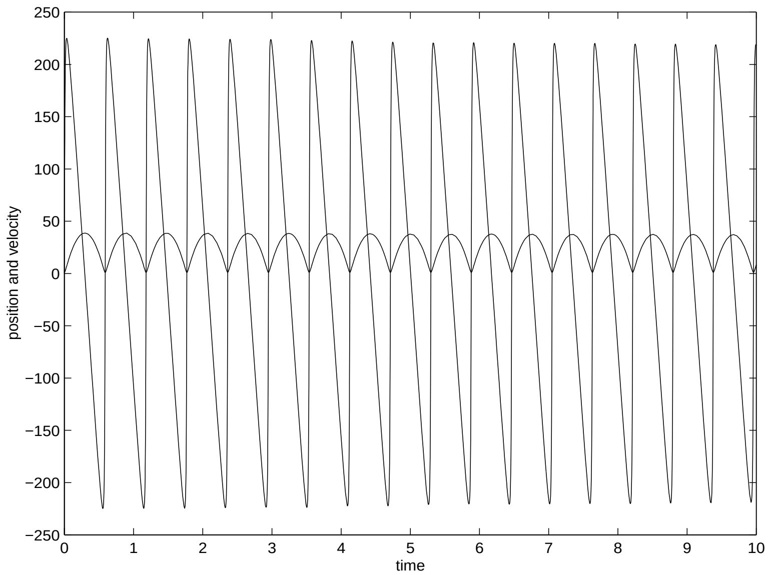

Figure 1: Position and velocity for a constant power.

A Lyapunov design consists of choosing u such that $-\dot{V}$ is positive definite. Then, we can solve for a family of controllers $u(x, V, \dot{V})$ as follows:

$$u(x, V, \dot{V}) = \frac{1}{G(x)}\left[g + \frac{\dot{V}(x) - \frac{\partial V(x)}{\partial x_1}x_2}{\frac{\partial V(x)}{\partial x_2}}\right]. \tag{14}$$

This particular input will stabilize the system to the origin. In general, however, we need to keep the sail at an elevation $x_1 = \bar{z}$ while the velocity is $x_2 = \dot{\bar{z}} = 0$. In order to accomodate this case, define the error system using $e_1 = x_1 - \bar{z}$ and $e_2 = \dot{e}_1 = x_2$. Using a similar approach, we obtain

$$u(e, V, \dot{V}) = \frac{1}{G(e)}\left[g + \frac{\dot{V}(e) - \frac{\partial V(e)}{\partial e_1}e_2}{\frac{\partial V(e)}{\partial e_2}}\right]. \tag{15}$$

3.2.2 Feedback-linearization design

For the system (13), and since $G(x) \neq 0$ for all x, we can use a feedback-linearization based controller [5] as follows:

$$u(e) = \frac{1}{G(e)}[g - K_1 e_1 - K_2 e_2], \tag{16}$$

where K_1 and K_2 are positive numbers that then make the closed-loop system stable with a characteristic polynomial $s^2 + K_2 s + K_1$. We can use the freedom in the choice of K_1 and K_2 to specify the closed-loop behavior of the system.

4 Numerical Example

In what follows, we illustrate the concepts of the 1-D model using a numerical example with the following values for system (1): Let $g = 918$ cm/s^2, $R = 1.59$ cm and consider first the case where P is a constant. Figure 1 illustrates the oscillating position and velocity and Figure 2 illustrate the phase plane plot for $P/P_0 = 2$. In Figure 3 we show the closed-loop behavior with the stabilizing controller (16), while Figure 4 shows the control effort.

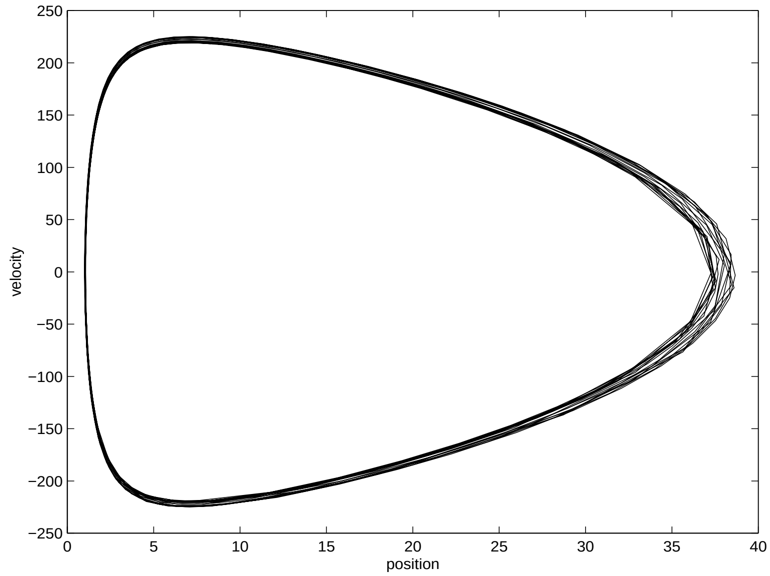

Figure 2: Position and velcoity phase plot for a constant power.

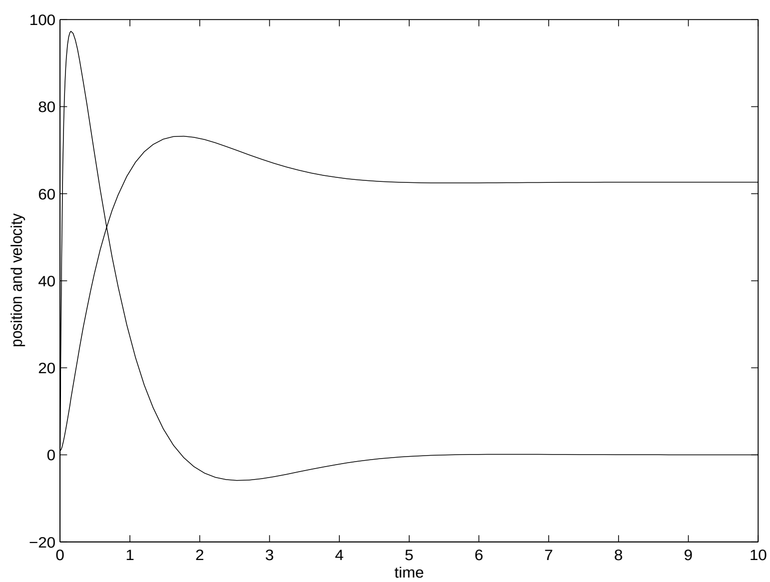

Figure 3: Position and velocity with feedback.

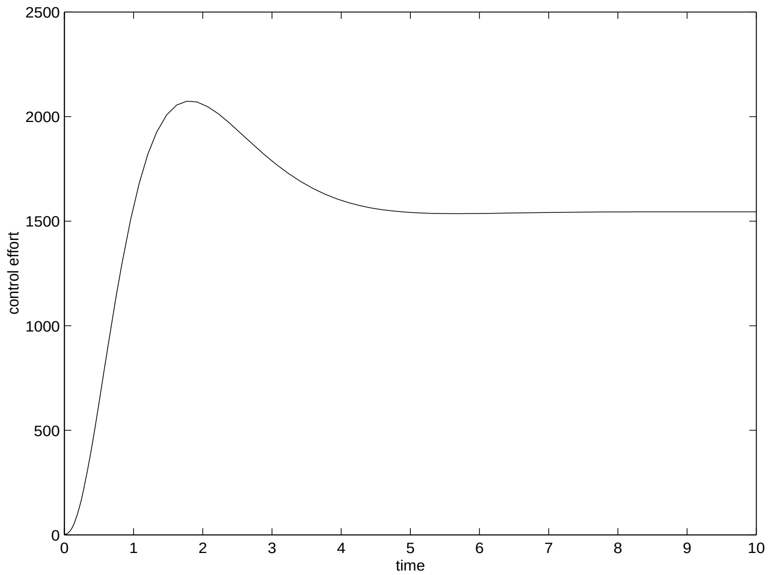

Figure 4: Feedback control effort.

5 3-D Problem Statement

The 3-dimensional dynamics are described by [6]:

$$\begin{aligned} \dot{r}_c &= v_c \\ \dot{q} &= \frac{1}{2} w \star q \\ \dot{v}_c &= \frac{F}{m} + G \\ \dot{w} &= J^{-1}\left[-w \times Jw + T\right] \end{aligned} \tag{17}$$

where r_c denotes the 3-dimensional inertial position vector of the vehicle center of mass, v_c the inertial velocity of the vehicle, q is the corresponding attitude quaternion of the body frame orientation in inertial coordinates, w the angular rate vector in body cordinates, F is the induced inertial force on the vehicle, T is the induced body torque, $G = [0 \ \ 0 \ \ -9.807] m/s^2$ is the gravity vector, m is the vehicle mass, J is the vehicle monent of inertia, and $\star$ is the quaternion multiplication operation. Let the state vector be x which is formed as follows:

$$x = \begin{bmatrix} x_1 \\ x_2 \\ x_3 \\ x_4 \\ \cdots \\ x_{10} \\ x_{11} \\ x_{12} \\ x_{13} \end{bmatrix} = \begin{bmatrix} r_c \\ q \\ v_c \\ w \end{bmatrix} \tag{18}$$

Note that F and T are of the form $F = \bar{f}(x)u$ and $T = \bar{t}(x)u$. Therefore, we can write the nonlinear dynamics in the form

$$\dot{x} = f(x) + g(x)u \tag{19}$$

When u is constant, we can analyze (19) as if it were an autonomous nonlinear systems given by

$$\dot{x} = f(x) \tag{20}$$

We can then study the stability of an equilibrum point of the system (20). In order to do we first find the equilbrium state

$$\begin{aligned} x_e &= [r_{ce} \;\; q_e \;\; v_{ce} \;\; w_e]^T \\ &= [0 \;\; 0 \;\; z_{eq} \;\; | \;\; 0 \;\; 0 \;\; 0 \;\; 1 \;\; | \;\; 0 \;\; 0 \;\; 0 \;\; | \;\; 0 \;\; 0 \;\; 0]^T \end{aligned} \tag{21}$$

and $T(x_e) = 0$, $F(x_e) = mG$. The question of stability of the equilibrium point x_e can not however be unambigously decided from linearization. The main problem occurs when the linearization of (20) about x_e leads to the system $\dot{x} = Ax$ where the some of the eigenvalues of A lie on the jw axis.

In order to study the stability of rigid concave sails numerically, a stand-alone dynamics simulation environment (written in the C programming language) was developed by Singh at JPL [6]. An umbrella-like configuration with an adequate center-of-mass/center-of-pressure offset) with its concave side facing the impinging microwave radiation is shown to be stable in translation and rotation. In this context, stability implies a bounded-motion behavior. The sail (also termed *vehicle* is modeled as a perfectly reflecting rigid body. Possible multiple reflections are not included in the model. The simulation environment is restricted to conical reflectors with a linear mast of appropriate length and mass tocreate the adequate center-of-mass/center-of-pressure offset (Maybe include a scanned figure here). The mast structure conincides with the vehicle's axis of symmetry. The vehicle shape is shown in figure 5.

This simulation was used to determine the stable parameter regime of the sail and then to study the region of attraction about the equilibrium points. Preliminary results will be included in the final version of the paper to illustrate some of our findings.

6 Conclusions

In this paper we have studied the control problem of a conical-shaped microwave-propelled sails in the 1-D case. It was shown that open-loop constant magnitude power control will leas to oscillatory behavior but that various closed-loop controllers may be designed to maintain the sail at any desired altitude.

We have also performed some 3-D simulations utilizing a simulation environment that was developed at JPL for studying conical sails with a linear mast. Further work utilizing this code will invoke concepts from statistical learning to assist with better identifying the parameters for studying the stability boundaries.

The approach advocated here will be next extended to the full 3-D problem. The dynamics in such a case are much more involved and have been derived numerically. Various laboratory experiments have been completed in order to understand the sails properties, and various simulations are underway in order to help in the control design.

References

[1] "Wireless Power Transmission for Science Applications," J. Benford, Microwave Sciences, Interim Final Report Contract number NAS8-99135, Microwave Sciences, 1041 Los Arabis Lane, Lafayette, CA 94549, May 2000.

[2] C. R. McInnes, *Solar Sailing: Technology, Dynamics, and Mission Applications* (Springer-Verlag, New York, 1999).

[3] J. Benford and R. Dickinson, "Space Propulsion and Power Beaming using Millimeter Systems," *Intense Microwave Pulses III, Proceedings SPIE*, vol. 2557, p. 179 (1995).

[4] H. K. Khalil, *Nonlinear Systems* (Prentice Hall, New Jersey, 1995).

[5] . A. Isiori, "Nonlinear Control Systems," 3rd Edition, Springer-Verlag, London, 1995.

[6] G. Singh, "Characterization of Passive Dynamic Stability of a Microwave Sail," *Jet Propulsion Laboratory Engineering Memorandum EM-3455-00-001*, 22 March 2000.

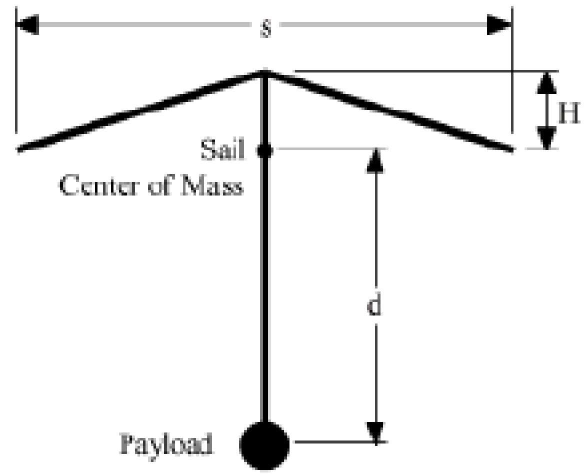

Circular Beam Rider
Stability Region:
Span = 10 cm, Height = 2 cm